

# BIFURCATIONS AND CANARDS IN TWO COUPLED FITZHUGH–NAGUMO EQUATIONS

March 18, 2025

BRUNO F.F. GONÇALVES, ISABEL S. LABOURIAU, AND ALEXANDRE A. P. RODRIGUES

**ABSTRACT.** We describe the slow-fast dynamics of two FitzHugh–Nagumo equations coupled symmetrically through the slow equations. We find an open set of parameter values for which the two equations synchronise, and another set with antisynchrony — where the solution of one equation is minus the solution of the other. We also obtain bistability — where these two types of solution coexist as attractors.

Canards are shown to give rise to mixed-mode oscillations. They also initiate small amplitude transient oscillations before the onset of large amplitude relaxation oscillations. We also discuss briefly the effect of asymmetric coupling, with periodic forcing of one of the equations by the other.

**Keywords:** FitzHugh–Nagumo; Symmetric Coupling; Bifurcations; Canards; Mixed Mode Oscillations.

**2020 Mathematics Subject Classification. Primary:** 34E15

**Secondary:** 34C60, 34E17, 34C15, 37G15

## 1. INTRODUCTION

Although the FitzHugh–Nagumo equations (FHN) were created as a simplified model for nerve impulse, they have also been intensively studied for purely mathematical reasons. This is because they provide a very simple example of equations that show complex and varied dynamics.

Several different formulations of the FitzHugh–Nagumo equations [8, 9, 21] occur in the literature both as reaction-diffusion equations and as ordinary differential equations. A review can be found in Cebrián-Lacasa *et al.* [3]. Here we see it as the slow-fast system of ordinary differential equations

$$(1) \quad \begin{cases} \varepsilon \dot{x} &= 4x - x^3 - y = f(x, y) \\ \dot{y} &= x - by - c = g(x, y) \end{cases} \quad b, c \in \mathbf{R} \quad 0 < \varepsilon \ll 1$$

where  $x$  is the fast variable and  $y$  is the slow one. Its dynamics was described in Gonçalves *et al.* [10]. In this article we explore the consequences of coupling two identical FHN.

Synchronisation of two coupled equations of Hodgkin-Huxley type (models for nerve impulse) has been studied by Labouriau & Rodrigues [20], but it does not cover FHN. Coupling two FHN has been addressed in many places in the literature. For instance, the effect of having the fast variable of a periodic solution of a FHN coupled to the fast equation of another FHN and thus forcing it has been explored numerically by several authors. It was described as experiments in an electrical circuit by Binczack *et al.* [1], through self-coupling by Desroches *et al.* [4] and also numerically by Hoff *et al.* [14]. Coupling FHN symmetrically through the fast equations has been also addressed both numerically and analytically in Pedersen *et al.* [22] and Kristiansen and Pedersen [16], numerically by Hoff *et al.* [14]. For both symmetric and asymmetric coupling through the fast equations, it is studied analytically by Campbell and Waite [2], numerically by Santana *et al.* [24] and with a delay in Saha and Freudel [23]. Two different coupling constants, one for the fast variables the other for the slow ones are explored by Kawato *et al.* [15] and by Krupa *et al.* in 2014 [17]. Other authors use the slow coordinate of a periodic solution of one FHN to force the fast coordinate of another, as in Doss-Bachelet *et al.* [5] and Krupa *et al.* in 2012 [18], the latter in a model with three time scales. Many of these authors explored the slow-fast structure of the equations focusing on several different aspects of the dynamics: synchrony, periodic and chaotic mixed-mode oscillations, canards, and bursts. We will discuss their findings in more detail in the final section of this article.

Here we couple two identical FHN symmetrically through the slow equations. To the best of our knowledge this has not been done before. The coupling may be understood as a diffusive term since it depends on the

difference of the slow variables, that in the original formulation of FHN represents ion transport through a membrane. It allows us to compare the different types of coupling, as discussed in Section 6 below.

**Structure of the article.** After describing the model in Section 2 and its critical manifold in Section 3 we discuss conditions where the solution of the two equations synchronise in Section 4. Canards, giving rise to mixed-mode oscillations and small amplitude transients, are treated in Section 5. Finally our results are discussed in Section 6 comparing them to the findings by the above mentioned authors, with pointers to future work, followed by a brief excursion into the possibly chaotic mixed-mode oscillations that arise in one-directional coupling where one FHN is used for periodically forcing the other.

We have endeavoured to make a self contained exposition bringing together all related topics. We have drawn illustrative figures to make the paper easily readable. All figures in this article were created through numerical simulations conducted in *Matlab*, using integration functions such as *ode15s* or *ode23s*, except for a figure drawn by the authors.

## 2. THE OBJECT OF STUDY

We study the dynamics of two FitzHugh–Nagumo equations coupled through the slow equations:

$$(2) \quad \begin{cases} \varepsilon \dot{x}_1 = -y_1 + \varphi(x_1) \\ \varepsilon \dot{x}_2 = -y_2 + \varphi(x_2) \\ \dot{y}_1 = x_1 - by_1 - c - k(y_1 - y_2) \\ \dot{y}_2 = x_2 - by_2 - c - k(y_2 - y_1) \end{cases} \quad \varphi(x) = 4x - x^3 \quad b, c, k \in \mathbf{R} \quad k \neq 0 \quad 0 < \varepsilon \ll 1 .$$

This is a simplified model for the study of a network of two Hodgkin-Huxley neurones, as in two identical coupled nerve cells with dynamics given by  $(x_1, y_1)$  and  $(x_2, y_2)$ . The parameter  $k \neq 0$  is the coupling strength.

The parameters  $b$  and  $c$  modulate the dynamics of each cell as discussed in [10] and in [3]. We think of (2) as two coupled cells, each one with dynamics represented by  $(x_1, y_1)$  and  $(x_2, y_2)$ . When  $k = 0$ , the two cells are independent and the dynamics of (2) is characterised by the cartesian product of two FitzHugh–Nagumo equations. As described in [10], the dynamics of a single FitzHugh–Nagumo model is characterised by the existence of at least one and at most three equilibrium states, that may be either stable, unstable or saddles. For some parameter values there is also a periodic solution. This implies that for  $k = 0$  (no coupling) the dynamics of (2) is characterised by the existence of periodic orbits (cartesian product with one of the equilibria) and by a resonant hyperbolic torus foliated by periodic solutions of rotation number 1. Hopf bifurcations and *canard explosions* have been found in the particular cases  $b = 0$  (cf. [10, Example 6.1]) and  $c = 0$  (cf. [10, Example 6.2]). For  $k \neq 0$  the dynamics of each oscillator interferes on the other. The normally hyperbolic torus (when it exists) persists for  $k > 0$  small.

System (2) is formulated as a slow-fast system with two fast and two slow equations that are, respectively, the equations for  $\dot{x}_i$  and for  $\dot{y}_i$ ,  $i = 1, 2$ . There is a huge literature on this type of system, we refer the reader to the book [19], whose treatment we follow.

Accordingly, we call  $X = (x_1, x_2)$  the *fast variables* whose dynamics is governed by the *fast equations*  $\varepsilon \dot{X} = F(X, Y)$  with  $Y = (y_1, y_2)$  and

$$F(x_1, x_2, y_1, y_2) = (-y_1 + \varphi(x_1), -y_2 + \varphi(x_2)) .$$

Similarly, the *slow variables*  $Y = (y_1, y_2)$  obey the *slow equations*  $\dot{Y} = G(X, Y)$  with

$$G(x_1, x_2, y_1, y_2) = (x_1 - by_1 - c - k(y_1 - y_2), x_2 - by_2 - c - k(y_2 - y_1)) .$$

## 3. THE CRITICAL MANIFOLD

An important concept in the dynamics of slow-fast systems is the *critical manifold*  $C_0$  defined as the set of equilibria of the fast equations. In the singular case  $\varepsilon = 0$  this is the manifold where solutions lie. In the present case it is the surface

$$C_0 = \{(x_1, x_2, y_1, y_2) \in \mathbf{R}^4 : y_i = \varphi(x_i), i = 1, 2\} ,$$

that contains the *fold lines* where its projection into the slow variables  $y_1, y_2$  is singular, i.e., where either  $\varphi'(x_1) = 0$  or  $\varphi'(x_2) = 0$ . The set of fold lines is given by

$$(3) \quad \Sigma = \{(x_1, x_2, y_1, y_2) \in C_0 : x_1 = \pm 2/\sqrt{3} \quad \text{or} \quad x_2 = \pm 2/\sqrt{3}\} .$$

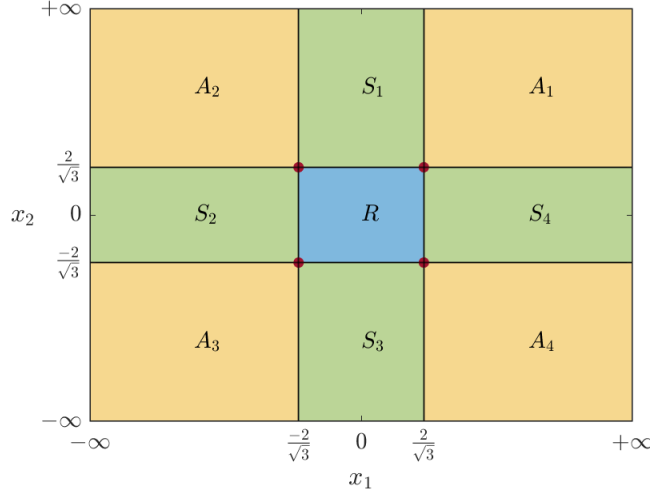


FIGURE 1. The critical manifold  $C_0$  projected into the  $(x_1, x_2)$  plane as in Lemma 3.2 with four attracting regions  $A_1 \cup A_2 \cup A_3 \cup A_4 = A$  (yellow), four saddle regions  $S_1 \cup S_2 \cup S_3 \cup S_4 = S$  (green) one repelling region  $R$  (blue), four fold lines (black) and four double fold points (red dots).

The degenerate points  $(x_1, x_2, \varphi(x_1), \varphi(x_2)) \in \Sigma$  with both  $x_1 = \pm x_2$  and  $x_1 = \pm 2/\sqrt{3}$  are *double folds*, that correspond to the transverse crossing of two fold lines in  $C_0$ .

**Definition 3.1.** Let  $v(\xi)$  be a smooth vector field in  $\mathbf{R}^n$ . A smooth manifold  $M \subset \mathbf{R}^n$  invariant under the flow of  $\dot{\xi} = v(\xi)$  is normally hyperbolic if there is a smooth splitting  $T\mathbf{R}^n|_M = TM \oplus N$  such that for all  $\xi \in M$  the eigenvalues of  $Dv(\xi)|_N$  have non-zero real part.

**Lemma 3.2.** The critical manifold  $C_0$  for (2) is normally hyperbolic with respect to the fast equations everywhere except at the fold points in  $\Sigma$ . The complement  $C_0 \setminus \Sigma$  has 9 connected components (see Figure 1) corresponding to the different types of stability of equilibria of the fast equations:

- four regions with attracting equilibria, their union is  $A = \{(x_1, x_2, y_1, y_2) : |x_i| > 2/\sqrt{3} \quad y_i = \varphi(x_i) \quad i = 1, 2\}$  where  $\partial F/\partial X$  has two eigenvalues with negative real part;
- four regions with saddle equilibria, their union is  $S = \{(x_1, x_2, y_1, y_2) : |x_i| - 2/\sqrt{3} \text{ have opposite signs and } y_i = \varphi(x_i) \quad i = 1, 2\}$  where  $\partial F/\partial X$  has two eigenvalues of opposite signs;
- one region with repelling equilibria  $R = \{(x_1, x_2, y_1, y_2) : |x_i| < 2/\sqrt{3} \quad y_i = \varphi(x_i) \quad i = 1, 2\}$  where  $\partial F/\partial X$  has two eigenvalues with positive real part.

The sets  $A$  and  $S$  of the previous result may be written as the disjoint union described in the caption of Figure 1.

*Proof.* The fast equations consist of a family of equations in the variables  $x_1$  and  $x_2$  parametrised by  $Y = (y_1, y_2)$ . In this context, for each  $Y$  the manifold  $C_0$  consists of isolated points, hence its tangent space is trivial and normal hyperbolicity reduces to the hyperbolicity of the equilibria of the fast equation. This is determined by the eigenvalues of the derivative of  $F(X, Y)$  with respect to the fast variables  $X$ , i.e. by the matrix

$$\frac{\partial F}{\partial X}(x_1, x_2, y_1, y_2) = \begin{pmatrix} \varphi'(x_1) & 0 \\ 0 & \varphi'(x_2) \end{pmatrix} \quad \text{where} \quad \varphi'(x) = 4 - 3x^2.$$

The result follows by inspection of the sign of  $\varphi'$ . □

**Definition 3.3.** A set  $S \subset \mathbf{R}^n$  is locally flow-invariant under a vector field  $W$  defined in  $\mathbf{R}^n$  if for every point  $x_0 \in S$  there is a  $t_0 > 0$  such that for every  $t$  with  $|t| < t_0$  the solution  $x(t)$  of differential equation  $\dot{x} = W(x)$  with  $x(0) = x_0$  lies in  $S$ .

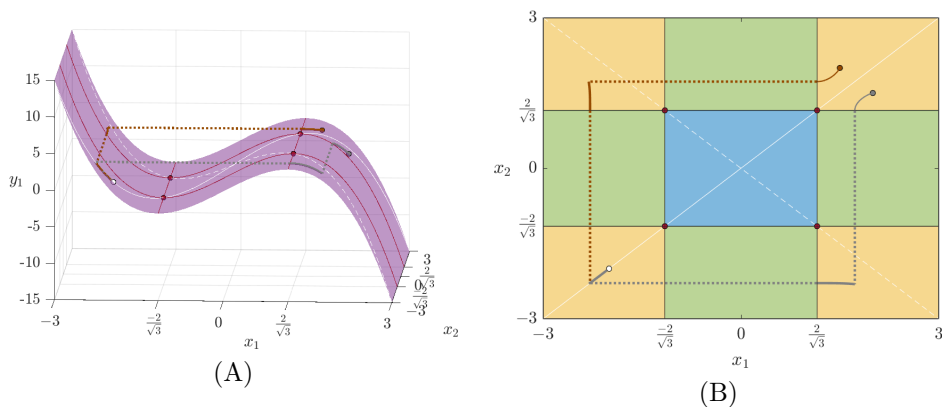


FIGURE 2. Two singular solutions of (2) attracted to the synchrony plane shown in two different projections, parameters  $b = 0, c = -2$  and  $k = 1$ . Conventions: trajectories with initial conditions at the brown and gray dots, slow part in brown/gray solid lines, fast part dotted, stable equilibrium (white dot), fold lines (red/black), double fold points (red dots), intersection with synchrony plane white line. (A) - Projection of  $C_0$  into the subspace  $(x_1, x_2, y_1)$  (purple). (B) - Same trajectories as in (A) projected into the plane  $(x_1, x_2)$ .

From Lemma 3.2 we obtain the following result:

**Corollary 3.4.** *For every  $r \geq 2$  and for sufficiently small  $\varepsilon > 0$  there is a flow-invariant slow manifold  $C_\varepsilon$  of class  $C^r$  which is  $\mathcal{O}(\varepsilon)$  close, in the Hausdorff topology, to the normally hyperbolic part of  $C_0$ , where  $\mathcal{O}$  stands for the usual Landau notation. Moreover, close to the set  $A$  where  $C_0$  attracts the fast flow, the manifold  $C_\varepsilon$  is also locally attracting for the fast equations in (2) and there is a locally attracting and locally flow-invariant manifold  $A_\varepsilon$ .*

*Proof.* Since the critical manifold  $C_0$  is normally hyperbolic everywhere except at the fold points in  $\Sigma$ , the result follows by Fenichel's Theorem [7].  $\square$

Thus, for small  $\varepsilon$  a typical solution of (2) behaves as follows: a trajectory starting away from  $C_\varepsilon$  moves fast to the attracting part,  $A_\varepsilon$ , of  $C_\varepsilon$  and remains near this sheet, with the dynamics close to that of the slow equations in  $C_0$ , until it runs into the fold line  $\Sigma$ . At  $\Sigma$  it will typically jump out of  $C_\varepsilon$  and move fast to another attracting component of  $C_\varepsilon$  close to  $C_0 \setminus \Sigma$ . Therefore, solutions of (2) for small  $\varepsilon > 0$  will be close to *singular solutions*, defined as trajectories that move with the fast equation into the attracting part of  $C_0$  and move on  $C_0$  following the slow equations.

In special situations a trajectory may cross  $\Sigma$  and remain in the unstable region of  $C_\varepsilon$  for some time. Such a trajectory is called a *canard* and will be discussed in Section 5 below.

#### 4. SYNCHRONY

Equations (2) have the symmetry  $\gamma(x_1, x_2, y_1, y_2) = (x_2, x_1, y_2, y_1)$ , therefore the plane

$$\{(x, x, y, y) \in \mathbf{R}^4\} = \text{Fix}(\gamma)$$

is flow-invariant. Solutions in this plane correspond to two synchronised cells: they behave like a single FitzHugh–Nagumo system. We refer to this plane as the *synchrony plane*. Equilibria in this plane satisfy both  $y = \varphi(x) = 4x - x^3$  and  $x - b\varphi(x) - c = 0$ . Therefore in  $\text{Fix}(\gamma)$  there is always at least one equilibrium and there are at most three equilibria — details in Section 3 of [10]. By the Bézout Theorem there are at most 9 equilibria of (2) so there may be up to 3 symmetry related pairs of equilibria outside the synchrony plane.

The symmetry implies that the synchrony plane  $\text{Fix}(\gamma)$  is invariant under the flow of (2). The next result provides conditions for its intersection with the attracting part,  $A$ , of  $C_0$  to be attracting.

**Proposition 4.1.** *The intersection  $\text{Fix}(\gamma) \cap A$  is normally hyperbolic if and only if  $b + 2k \geq 0$ . Moreover, in this case it is locally attracting.*

*Proof.* The normal hyperbolicity of the invariant plane  $\text{Fix}(\gamma)$  is determined by the eigenvalues of the component  $N$  of the derivative of the vector field  $V(X, Y) = (F(X, Y), G(X, Y))$  transverse to  $\text{Fix}(\gamma)$ . We change

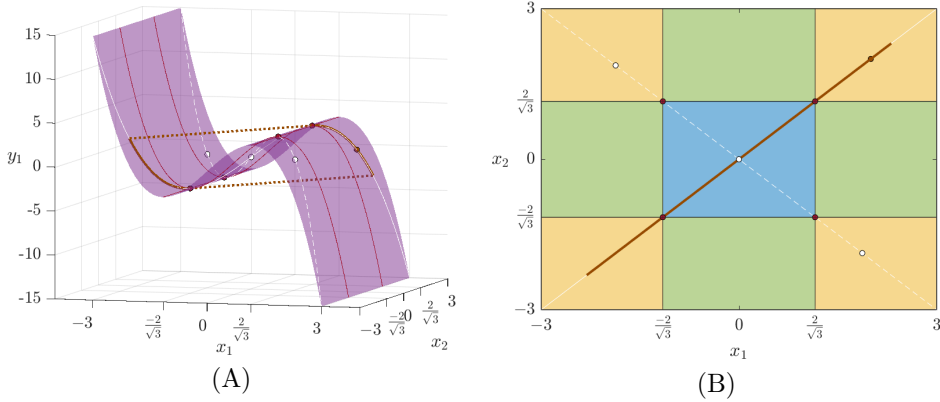


FIGURE 3. Singular solution of (2) on the synchrony plane shown in two different projections, parameters  $b = 0 = c$  and  $k = 1$ . Conventions: trajectories with initial conditions at the brown dot, slow part in brown solid lines, fast part dotted, equilibria (white dots), fold lines (red/black) degenerate fold points (red dots), intersection with synchrony plane (white line). (A) - Projection  $C_0$  into the subspace  $(x_1, x_2, y_1)$  (purple). (B) - Same trajectories as in (A) projected into the plane  $(x_1, x_2)$ .

coordinates to  $z_1 = x_1 + x_2$ ,  $z_2 = y_1 + y_2$  in  $\text{Fix}(\gamma)$  and  $z_3 = x_1 - x_2$ ,  $z_4 = y_1 - y_2$  in  $\text{Fix}(\gamma)^\perp$ , the orthogonal complement of  $\text{Fix}(\gamma)$ . This means that:

$$x_1 = \frac{z_1 + z_3}{2}, \quad x_2 = \frac{z_1 - z_3}{2}, \quad y_1 = \frac{z_2 + z_4}{2} \quad \text{and} \quad y_2 = \frac{z_2 - z_4}{2}.$$

Let  $\widehat{V}(Z)$  be the expression of the vector field  $V(X, Y)$  in the new coordinates  $Z = (z_1, z_2, z_3, z_4)$ , with associated equations given by

$$(4) \quad \begin{cases} \varepsilon \dot{z}_1 &= -z_2 + \varphi\left(\frac{z_1 + z_3}{2}\right) + \varphi\left(\frac{z_1 - z_3}{2}\right) \\ \dot{z}_2 &= z_1 - bz_2 - 2c \\ \varepsilon \dot{z}_3 &= -z_4 + \varphi\left(\frac{z_1 + z_3}{2}\right) - \varphi\left(\frac{z_1 - z_3}{2}\right) \\ \dot{z}_4 &= z_3 - bz_4 - 2kz_4. \end{cases}$$

Computing  $D\widehat{V}(Z)$  at the plane  $\text{Fix}(\gamma)$ , given by  $x_1 = x_2 = x$ ,  $y_1 = y_2 = y$  where  $z_1 = 2x$ ,  $z_2 = 2y$ ,  $z_3 = z_4 = 0$  we obtain:

$$(5) \quad D\widehat{V}(z_1, z_2, z_3, z_4) \Big|_{(2x, 2y, 0, 0)} = \begin{pmatrix} \varphi'(x) & -1 & 0 & 0 \\ 1 & -b & 0 & 0 \\ 0 & 0 & \varphi'(x) & -1 \\ 0 & 0 & 1 & -(b+2k) \end{pmatrix} \quad N_\gamma = \begin{pmatrix} \varphi'(x) & -1 \\ 1 & -(b+2k) \end{pmatrix}$$

where  $N_\gamma$  is the component of  $D\widehat{V}(Z)$  in the directions perpendicular to  $\text{Fix}(\gamma)$ , evaluated at  $Z = (2x, 2y, 0, 0) \in \text{Fix}(\gamma)$ .

The synchrony plane is attracting if  $\det(N_\gamma) > 0$  and  $\text{Tr}(N_\gamma) < 0$  where

$$\det(N_\gamma) = -(b+2k)\varphi'(x) + 1 \quad \text{and} \quad \text{Tr}(N_\gamma) = \varphi'(x) - (b+2k).$$

As we saw in Section 3, points in the critical manifold attract the fast flow if  $\varphi'(x_i) < 0$  for  $i = 1, 2$ . So, if  $b+2k \geq 0$  then  $\text{Fix}(\gamma) \cap A$  is normally hyperbolic and attracting, since  $\det(N_\gamma) > 0$  and  $\text{Tr}(N_\gamma) < 0$ .

Finally, to see that the condition  $b+2k \geq 0$  is necessary for  $\text{Fix}(\gamma)$  to be normally hyperbolic, note that in  $\text{Fix}(\gamma) \cap A$  the derivative  $\varphi'(x) = 4 - 3x^2$  takes all values in the interval  $(-\infty, 0)$ . Therefore, if  $b+2k < 0$  there will be some point in  $\text{Fix}(\gamma) \cap A_\varepsilon$  where  $\varphi'(x) = 1/(b+2k)$ , hence  $\det(N_\gamma) = 0$ . At this point 0 is an eigenvalue of  $N_\gamma$ , so normal hyperbolicity fails. Moreover, there will also be some points where either  $\text{Tr}(N_\gamma) > 0$ , or where  $\det(N_\gamma) < 0$ , so some trajectories contained in this set may be attracting, but not all of them.  $\square$

It remains to see whether the intersection of the the synchrony plane with the attracting part,  $A_\varepsilon$ , of  $C_\varepsilon$  is also attracting.

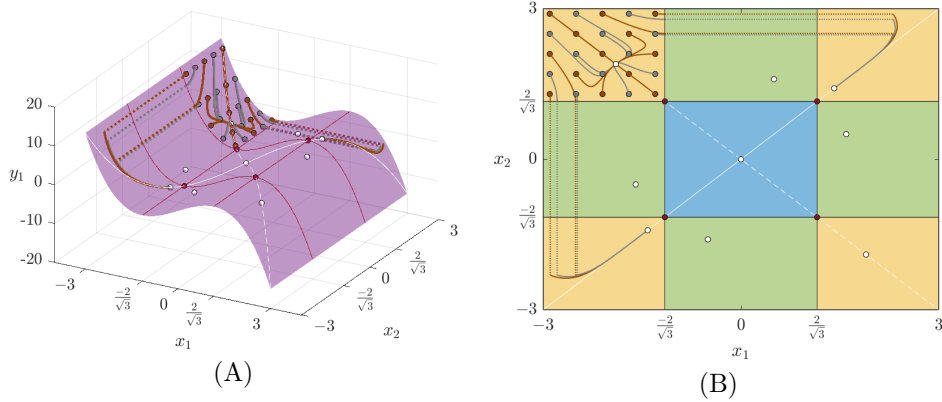


FIGURE 4. Several singular solutions of (2) starting in region  $A_2$  shown in two different projections, parameters  $b = 0.5$ ,  $c = 0$  and  $k = 1$ . Trajectories starting close to the fold line are attracted to the synchrony plane; other trajectories go to  $\text{Fix}(\delta)$ . Conventions: trajectories with initial conditions at the brown and gray dots, slow part in brown/gray solid lines, fast part dotted lines, equilibria white dots, fold lines (red/black), double fold points red dots, intersection with synchrony/anti-synchrony planes (solid/dotted lines, respectively). (A) - Projection of  $C_0$  into the subspace  $(x_1, x_2, y_1)$  (purple) and trajectories. (B) - Same trajectories as in (A) projected into the plane  $(x_1, x_2)$ .

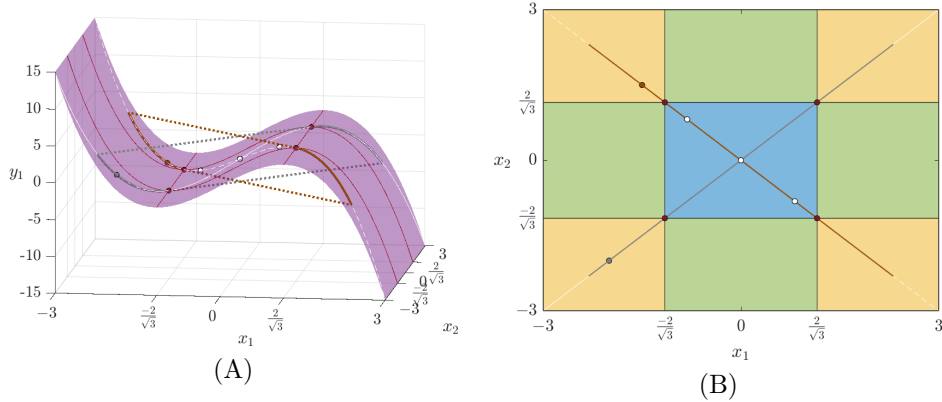


FIGURE 5. Two singular solutions of (2) starting in  $\text{Fix}(\gamma) \cap A_2$  and in  $\text{Fix}(\delta) \cap A_3$  shown in two different projections, parameters  $b = 0.1$ ,  $c = 0$  and  $k = 0.1$ . Two distinct stable solutions - bistability. Conventions: trajectories with initial conditions at the brown and gray dots, slow part in brown/gray solid lines, fast part dotted lines, equilibria g white dots, fold lines (red/black), double fold points red dots, intersection with synchrony/anti-synchrony planes (solid/dotted lines), respectively. (A) - Projection of  $C_0$  into the subspace  $(x_1, x_2, y_1)$  (purple) and trajectories. (B) - Same trajectories as in (A) projected into the plane  $(x_1, x_2)$ .

**Proposition 4.2.** *For small  $\varepsilon > 0$  the intersection  $\text{Fix}(\gamma) \cap A_\varepsilon$  is locally flow-invariant under (2). It is normally hyperbolic and locally attracting if  $b + 2k \geq 0$ .*

*Proof.* Since  $\gamma$  is a symmetry of (2) then the synchrony plane  $\text{Fix}(\gamma)$  is flow-invariant. By Corollary 3.4 the attracting part  $A_\varepsilon$  of the manifold  $C_\varepsilon$  is locally flow-invariant. Since both  $\text{Fix}(\gamma)$  and  $C_\varepsilon$  are locally flow-invariant sets, their intersection has the same property.

In the proof of Proposition 4.1 it is shown that if  $b + 2k \geq 0$  then, at any point  $Z \in \text{Fix}(\gamma) \cap A$ , the component  $N_\gamma(Z)$  of  $D\hat{V}(Z)$  perpendicular to  $\text{Fix}(\gamma)$  satisfies  $\det(N_\gamma)(Z) > 1$  and  $\text{Tr}(N_\gamma)(Z) < 0$ . From Corollary 3.4 we know that  $A_\varepsilon$  is  $\mathcal{O}(\varepsilon)$  close to  $A$ . Therefore, for small enough  $\varepsilon$ , if  $\tilde{Z} \in \text{Fix}(\gamma) \cap A_\varepsilon$ , then  $\det(N_\gamma)(\tilde{Z}) > 0$  and  $\text{Tr}(N_\gamma)(\tilde{Z}) < 0$  and the second statement follows.  $\square$

Proposition 4.2 is illustrated in Figures 2, 3, 4 and 5. Figures 4 and 5 illustrate the meaning of locally attracting: the synchrony plane attracts trajectories in an open set around it, but not all trajectories. In the example of the figures  $c = 0$ , hence (2) has additional symmetry and this is explored in the next result.

**Proposition 4.3.** *If  $c = 0$ , then the equations (2) have the additional symmetry*

$$\delta(x_1, x_2, y_1, y_2) = (-x_2, -x_1, -y_2, -y_1).$$

*The intersection  $\text{Fix}(\delta) \cap A$  is flow-invariant and it is normally hyperbolic if and only if  $b \geq 0$  and in this case it is locally attracting. Moreover, for small  $\varepsilon \geq 0$  the intersection  $\text{Fix}(\delta) \cap A_\varepsilon$  is locally flow-invariant, normally hyperbolic and locally attracting if  $b \geq 0$ .*

*Proof.* The plane  $\{(x, -x, y, -y)\} = \text{Fix}(\delta)$  is flow-invariant since it is fixed by the additional symmetry  $\delta$ . It remains to check that it is normally hyperbolic and to see where it is attracting. In the coordinates  $z_j$  used in the proof of Proposition 4.1 the subspace  $\text{Fix}(\delta)$  is defined by the equalities  $z_1 = z_2 = 0$ ,  $z_3 = 2x$  and  $z_4 = 2y$ . The expressions for the two matrices  $D\widehat{V}(z_1, z_2, z_3, z_4)\Big|_{(2x, 2y, 0, 0)}$  and  $D\widehat{V}(z_1, z_2, z_3, z_4)\Big|_{(0, 0, 2x, 2y)}$  are the same.

Hence, the component  $N_\delta$  of  $D\widehat{V}$  in the directions perpendicular to  $\text{Fix}(\delta)$  is given by:

$$N_\delta = \begin{pmatrix} \varphi'(x) & -1 \\ 1 & -b \end{pmatrix}$$

and then

$$\det(N_\delta) = -b\varphi'(x) + 1 \quad \text{and} \quad \text{Tr}(N_\delta) = \varphi'(x) - b.$$

Using the arguments of the proof of Proposition 4.1 it follows that  $\text{Fix}(\delta) \cap A$  is normally hyperbolic if and only if  $b \geq 0$  and in this case it is locally attracting. The last statement follows from the same arguments as Proposition 4.2.  $\square$

When  $c = 0$ , solutions of (2) that lie in the invariant plane  $\text{Fix}(\delta)$  satisfy  $(x_2(t), y_2(t)) = -(x_1(t), y_1(t))$ . We say they correspond to two cells with *antisynchrony*.

It follows from Propositions 4.1 and 4.3 that if  $c = 0$  and both  $b > 0$  and  $b + 2k > 0$  there is *bistability* i.e., the system has two stable coexisting states. In particular if  $0 < b < 1/4$  and  $c = 0$  then the uncoupled FHN in equations (1) have an asymptotically stable periodic solution, as established in [10]. In this case, provided  $b + 2k > 0$ , then (2) has two stable periodic solutions each one lying in one of the fixed-point subspaces for the two symmetries. Moreover, the bistability persists as shown in the next result.

**Corollary 4.4.** *If  $b > 0$  then for sufficiently small  $c \neq 0$  and for every  $r > 0$  there is a  $C^r$  locally flow-invariant locally attracting manifold for (2) close to  $\text{Fix}(\delta) \cap A_\varepsilon$ . If moreover  $b + 2k > 0$  there is bistability in the sense that the two locally invariant manifolds  $\text{Fix}(\delta) \cap A_\varepsilon$  and  $\text{Fix}(\gamma) \cap A_\varepsilon$  are locally attracting.*

*Proof.* The result follows from the normal hyperbolicity of Propositions 4.1 and 4.3 and Proposition 4.2 and from the persistence of normally hyperbolic locally invariant manifolds proved by Fenichel in [6] (see also [19, Section 2.2]).  $\square$

Similarly, from the persistence of normally hyperbolic invariant manifolds we obtain:

**Corollary 4.5.** *Consider a perturbation of (2) where the equation for  $\dot{y}_2$  is replaced by*

$$\dot{y}_2 = x_2 - \tilde{b}y_2 - \tilde{c} - \tilde{k}(y_2 - y_1) .$$

*Then for sufficiently small  $|b - \tilde{b}|$ ,  $|c - \tilde{c}|$  and  $|k - \tilde{k}|$  if  $b + 2k > 0$  and  $\tilde{b} + 2\tilde{k} > 0$ , there is an attracting normally hyperbolic locally invariant manifold for the perturbed system close to  $\text{Fix}(\gamma) \cap A_\varepsilon$ . In other words, the perturbed system has stable solutions with the two cells approximately synchronised. Moreover if  $b > 0$  and  $\tilde{b} > 0$  then, for sufficiently small  $c$  and  $\tilde{c}$ , the perturbed system has an attracting normally hyperbolic locally invariant manifold close to  $\text{Fix}(\delta) \cap A_\varepsilon$ , and hence it has bistability.*

## 5. CANARDS AND MIXED-MODE OSCILLATIONS

As remarked in Section 3 trajectories called *canards* may follow the unstable part of the slow manifold for a considerable amount of time. In geometric terms a canard solution corresponds to the intersection of an attracting and a repelling slow manifold near a non-hyperbolic point of  $\Sigma$ , the set of fold lines defined in (3). In this section, we establish some hypotheses ensuring the existence of canards for (2).

**Definition 5.1.** *A trajectory that, after starting  $\mathcal{O}(\varepsilon)$  close to the attracting region of the slow manifold, remains  $\mathcal{O}(\varepsilon)$  close to the non-attracting region of the slow manifold for a time of order  $\mathcal{O}(1)$  is called a canard.*

Szmolyan & Wechselberger [25] and Krupa *et al.* [17] have established that canards appear around some points where, after a rescaling that we will describe below, the slow equations have an equilibrium at a fold point.

In order to find the canards we start by rewriting the slow equations in terms of the fast variables by differentiating implicitly the condition  $y_i = \varphi(x_i)$ ,  $i \in \{1, 2\}$  that defines the critical manifold, to yield

$$(6) \quad \varphi'(x_i)\dot{x}_i = \dot{y}_i = x_i - (b+k)\varphi(x_i) + k\varphi(x_j) - c \quad i, j \in \{1, 2\}, \quad i \neq j.$$

A point  $X^* = (x_1^*, x_2^*, y_1^*, y_2^*)$  lies on the fold line  $\Sigma$  if and only if either  $\varphi'(x_1^*) = 0$  or  $\varphi'(x_2^*) = 0$ . Without loss of generality we take  $\varphi'(x_1^*) \neq 0$  and  $\varphi'(x_2^*) = 0$ , hence  $x_2^* = 2\sigma/\sqrt{3}$ ,  $\sigma = \pm 1$ , the case  $\varphi'(x_1^*) = 0$  and  $\varphi'(x_2^*) \neq 0$  being identical, due to the symmetry. The case  $\varphi'(x_1^*) = 0 = \varphi'(x_2^*)$  is treated separately at 5.2 below.

Since  $\varphi'(x_2^*) = 0$ , the equation obtained from  $\dot{y}_2$  in (6) yields no dynamical information at  $x_2 = x_2^*$ . We overcome this by a time rescaling of  $\tau = t/\varphi'(x_2)$ , that is singular at  $x_2^*$ , as mentioned above. Writing  $dx_i/d\tau = x'_i$  the equations (6) transform into:

$$(7) \quad \begin{cases} x'_1 &= \frac{\varphi'(x_2)}{\varphi'(x_1)}(x_1 - (b+k)\varphi(x_1) + k\varphi(x_2) - c) &= H_1(x_1, x_2) \\ x'_2 &= x_2 - (b+k)\varphi(x_2) + k\varphi(x_1) - c &= H_2(x_1, x_2). \end{cases}$$

The choice  $x_2^* = 2\sigma/\sqrt{3}$  imposes conditions on  $x_1^*$  as shown in the next result.

**Lemma 5.2.** *For every  $k \neq 0$  and for any choice of the parameters  $b$  and  $c$  there is an equilibrium  $(x_1^*, x_2^*)$  of (7) with  $x_2^* = 2\sigma/\sqrt{3}$ ,  $\sigma = \pm 1$  and  $|x_1^*| > \frac{2}{\sqrt{3}}$ . Therefore the point  $X^* = (x_1^*, x_2^*, \varphi(x_1^*), \varphi(x_2^*))$  lies at the boundary of the attracting part  $A$  of  $C_0$ .*

*Proof.* At  $x_2^* = 2\sigma/\sqrt{3}$  we have  $\varphi'(x_2^*) = 0$  so  $x'_1 = 0$ . Therefore  $(x_1^*, 2\sigma/\sqrt{3})$ ,  $\sigma = \pm 1$ , is an equilibrium of (7) if and only if  $x'_2 = 0$  i.e. when

$$(8) \quad k\varphi(x_1^*) = c + (b+k)\varphi\left(\frac{2\sigma}{\sqrt{3}}\right) - 2\sigma/\sqrt{3}$$

and the result follows immediately since for  $|x| > \frac{2}{\sqrt{3}}$  the function  $\varphi(x)$  takes all the values in  $\mathbf{R}$ .  $\square$

Note that an equilibrium  $(x_1^*, x_2^*)$  of (7) may *not* correspond to an equilibrium  $X^* = (x_1^*, x_2^*, \varphi(x_1^*), \varphi(x_2^*))$  of the original equations (2). Lemma 5.2 shows that there is an open set of parameters  $(k, b, c)$  of (2) such that there is an equilibrium  $(x_1^*, x_2^*)$  of (7) for which the point  $(x_1^*, x_2^*, \varphi(x_1^*), \varphi(x_2^*))$  lies at the boundary of the attracting set  $A$ .

The time rescaling that we have used allows us to gain enough hyperbolicity to obtain a complete analysis by standard methods from dynamical systems theory. We call the point  $(x_1^*, x_2^*)$  obtained in Lemma 5.2 a *folded equilibrium* of (7).

**Lemma 5.3.** *For  $k \neq 0$ , a folded equilibrium  $(x_1^*, 2\sigma/\sqrt{3})$ , with  $\sigma = \pm 1$ , of the equation (7) is either a saddle or an unstable node or an unstable focus or a saddle-node. For an open set of the parameters  $(k, b, c)$  it is either a saddle or an unstable node.*

*Proof.* For  $H(x_1, x_2) = (H_1(x_1, x_2), H_2(x_1, x_2))$  the derivative  $DH(x_1, x_2)$  at a folded equilibrium  $(x_1^*, x_2^*)$ ,  $x_2^* = 2\sigma/\sqrt{3}$ ,  $\sigma = \pm 1$ , of (7) is given by

$$(9) \quad DH(x_1^*, x_2^*) = \begin{pmatrix} 0 & \frac{\varphi''(x_2^*)}{\varphi'(x_1^*)}(x_1^* - (b+k)\varphi(x_1^*) + k\varphi(x_2^*) - c) \\ k\varphi'(x_1^*) & 1 \end{pmatrix}.$$

Therefore  $(x_1^*, x_2^*)$  is either a saddle or an unstable node or an unstable focus or a saddle-node for (7) since at least one of the eigenvalues is either positive or has positive real part because  $\text{Tr } DH(x_1^*, x_2^*) = 1$ .

The point  $(x_1^*, x_2^*)$  is either a saddle or an unstable node if and only if the eigenvalues of  $DH(x_1^*, x_2^*)$  are real and not zero, i.e., when  $0 \neq \det DH(x_1^*, x_2^*) \leq 1/4$ . From (9), we have:

$$\det DH(x_1^*, x_2^*) = -k\varphi''(x_2^*)(x_1^* - (b+k)\varphi(x_1^*) + k\varphi(x_2^*) - c).$$



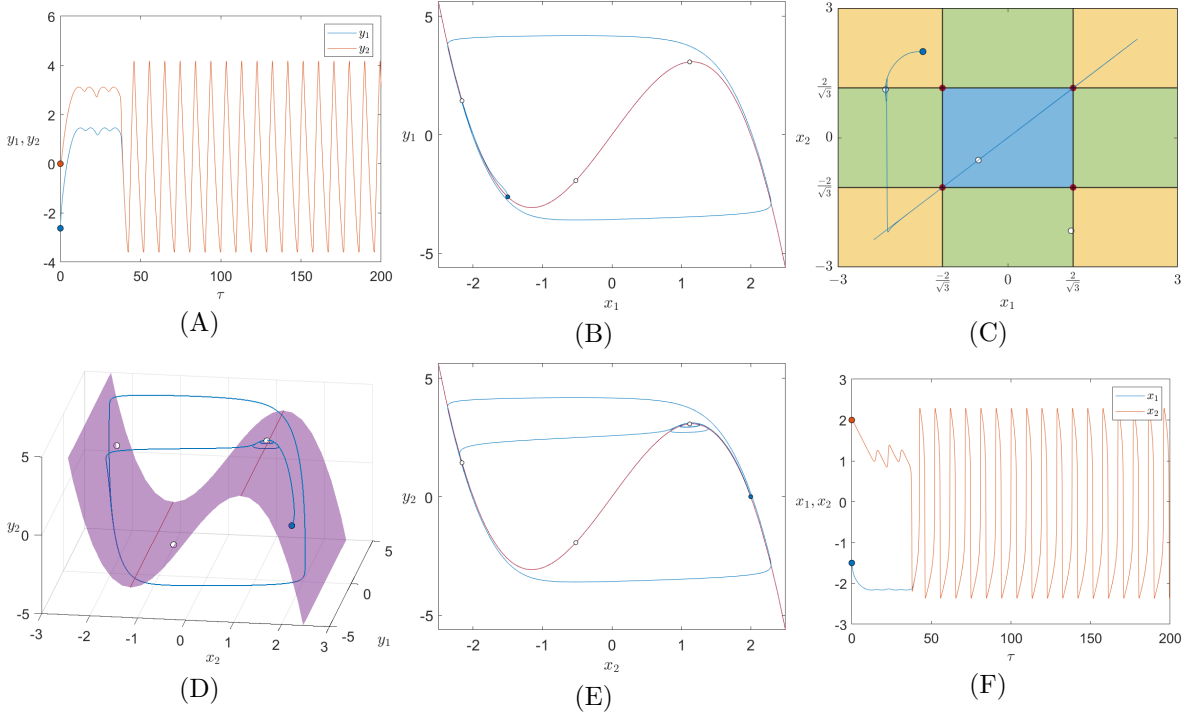


FIGURE 6. Canard transient on a solution of (2) near a folded node, parameters  $b = 0$ ,  $c = -0.519935054$ ,  $k = 1$  and  $\varepsilon = 0.5$ , initial condition  $(x_1, x_2, y_1, y_2) = (-1.5, 2, \varphi(-1.5), \varphi(2))$ . (A) - Time course for  $y_1(t)$  (blue) and  $y_2(t)$  (orange). (B) - Projection of the trajectory (blue) on the  $(x_1, y_1)$  plane, initial condition on the blue dot, red critical manifold  $C_0$ . (C) Projection of the trajectory (red) on the  $(x_1, x_2)$  plane, initial condition on the red dot, equilibria on the white dots. (D) - Projection of the trajectory (purple) on the  $(x_2, y_1, y_2)$  space, initial condition on the blue dot, purple critical manifold  $C_0$ . (E) - Projection of the trajectory (blue) on the  $(x_2, y_2)$  plane, conventions as in (B). (F) - Time course for  $x_1(t)$  (blue) and  $x_2(t)$  (orange).

Replacing  $\varphi(x_1^*)$  by the value in (8) the previous equality implies

$$(10) \quad \det DH(x_1^*, x_2^*) = -k\varphi''(x_2^*) [x_1^* + x_2^* - b(\varphi(x_1^*) + \varphi(x_2^*)) - 2c]$$

which is not zero and less than  $1/4$  for an open set of parameters  $(k, b, c)$ , since  $\varphi''(x_2^*) = -6x_2^* \neq 0$ .  $\square$

The time rescaling we have used reverses time orientation when  $(x_1^*, x_2^*, \varphi(x_1^*), \varphi(x_2^*))$  is in the attracting part of  $C_0$  where  $\varphi'(x_2^*) < 0$ , so when  $(x_1^*, x_2^*)$  is either a saddle or an unstable node for (7) there is at least one trajectory of (2) that goes across  $(x_1^*, x_2^*, \varphi(x_1^*), \varphi(x_2^*))$  generating a canard. This is a consequence of Lemma 2.3 of [25], where it is shown that canards correspond to, at least, one negative eigenvalue of (7). See also Guckenheimer & Haiduc [12] and Guckenheimer [13]. Examples are shown in Figures 6, 7 and 8.

In the first of these examples, before the trajectory approaches a synchronous periodic orbit it makes some transient small oscillations around the fold point that are visible in Figure 6 (E). In this example there is a folded node, see Table 1.

Note that from equation (10) it follows that for any given  $k \neq 0$  and  $b \in \mathbf{R}$  there is a value of the parameter  $c \in \mathbf{R}$  for which  $\det DH(x_1^*, x_2^*) = 0$ . This corresponds to saddle-node bifurcations. According to [17] this gives rise to mixed-mode oscillations like those shown in Figures 7 and 8, i.e., trajectories that combine small oscillations and large oscillations of relaxation type, both recurring in an alternating manner, cf. [17].

**5.1. The case  $b = 0$ .** More information on the equilibria of the equation (7) may be obtained if we make the simplifying assumption  $b = 0$ . Indeed the expression of (1) in the particular case  $b = 0$  has been used in the analysis of two FHN coupled in the fast equations by Pedersen *et al.* [22] and with double coupling fast-to-fast and slow-to-slow by Krupa *et al.* 2014 [17]. Thus this particular case is interesting for comparing the outcomes of different types of couplings.

From expression (8) the folded equilibrium  $(x_1^*, x_2^*)$  of (7) with  $x_2^* = 2\sigma/\sqrt{3}$ ,  $\sigma = \pm 1$ , satisfies the equality

$$(11) \quad k(\varphi(x_1^*) - \varphi(x_2^*)) = c - x_2^*.$$

Substituting into (10) we get

$$(12) \quad \det DH(x_1^*, x_2^*) = -k\varphi''(x_2^*)(x_1^* - k\varphi(x_1^*) + k\varphi(x_2^*) - c) = -k\varphi''(x_2^*)[x_1^* + x_2^* - 2c].$$

The folded equilibria  $(x_1^*, 2\sigma/\sqrt{3})$  may then be classified, in some cases under additional conditions on the sign of  $\varphi(x_2^*) - \varphi(x_1^*)$ , as shown in Table 1. To do this we divide the region  $A$  in four components  $A = A_1 \cup A_2 \cup A_3 \cup A_4$ , as depicted in Figure 1, where:

$$\begin{aligned} A_1 &= \left\{ (x_1, x_2, y_1, y_2) : x_1 > 2/\sqrt{3}, \quad x_2 > 2/\sqrt{3}, \quad y_i = \varphi(x_i), \quad i = 1, 2 \right\} \\ A_2 &= \left\{ (x_1, x_2, y_1, y_2) : x_1 < -2/\sqrt{3}, \quad x_2 > 2/\sqrt{3}, \quad y_i = \varphi(x_i), \quad i = 1, 2 \right\} \\ A_3 &= \left\{ (x_1, x_2, y_1, y_2) : x_1 < -2/\sqrt{3}, \quad x_2 < -2/\sqrt{3}, \quad y_i = \varphi(x_i), \quad i = 1, 2 \right\} \\ A_4 &= \left\{ (x_1, x_2, y_1, y_2) : x_1 > 2/\sqrt{3}, \quad x_2 < -2/\sqrt{3}, \quad y_i = \varphi(x_i), \quad i = 1, 2 \right\}. \end{aligned}$$

We will use the notation  $A_i^*$  for the sets  $A_i^* = \{(x_1, x_2) : (x_1, x_2, \varphi(x_1), \varphi(x_2)) \in A_i\}$ ,  $i = 1, \dots, 4$ .

In Table 1, we present sufficient conditions on  $c$  for the existence and classification of a folded equilibrium of (7) with  $b = 0$  on the components with  $x_2^* = \pm 2/\sqrt{3}$  of  $\partial A_i^*$ ,  $i = 1, \dots, 4$ , the boundary of the attracting region of the critical manifold. The analysis for folded equilibria with  $x_2^* = \pm 2/\sqrt{3}$  follows by symmetry. We present the computations for the cases where the folded equilibrium  $(x_1^*, x_2^*)$  lies on the boundaries of  $A_1^*$  and  $A_2^*$ . The computations for the other cases in Table 1 run along the same lines. For  $(x_1^*, x_2^*) \in \partial A_1^*$  and  $\partial A_3^*$  the classification is simpler, since  $\varphi(x_1^*) - \varphi(x_2^*)$  has constant sign.

**Case  $\partial A_1^*$ .** If the folded equilibrium  $(x_1^*, x_2^*) = (x_1^*, 2/\sqrt{3})$  lies on the boundary,  $\partial A_1^*$ , of region  $A_1^*$  then the following conditions hold:

$$\varphi''(x_2^*) = -6x_2^* < 0 \quad x_1^* - x_2^* > 0 \quad x_1^* + x_2^* > 4/\sqrt{3} > 0 \quad \varphi(x_1^*) - \varphi(x_2^*) < 0.$$

We start by obtaining sufficient conditions on the parameter  $c$  for the existence of a folded equilibrium, and then proceed to classify it:

- (1) If  $c < 2/\sqrt{3} = x_2^*$  then (11) implies that  $k > 0$ . Therefore  $\det H(x_1^*, x_2^*) = -k\varphi''(x_2^*)[x_1^* + x_2^* - 2c] > 0$ , and hence  $(x_1^*, x_2^*)$  is either a node or an unstable focus of (7).
- (2) If  $c > 2/\sqrt{3} = x_2^*$ , then (11) implies that  $k < 0$ . In this case there are the following possibilities:
  - (a) If  $c > (x_1^* + 2/\sqrt{3})/2$  then  $\det H(x_1^*, x_2^*) > 0$  and  $(x_1^*, x_2^*)$  is either a node or an unstable focus of (7).
  - (b) If  $c < (x_1^* + 2/\sqrt{3})/2$  then  $\det H(x_1^*, x_2^*) > 0$  and  $(x_1^*, x_2^*)$  is a saddle.

**Case  $\partial A_2^*$ .** Similarly to what we did before, if the folded equilibrium  $(x_1^*, x_2^*) = (x_1^*, 2/\sqrt{3})$  lies on the boundary,  $\partial A_2^*$ , of region  $A_2^*$  then we have

$$\varphi''(x_2^*) = -6x_2^* < 0 \quad x_1^* < -2/\sqrt{3} = -x_2^*.$$

We divide the calculation in two main cases:

- (1) If  $\varphi(x_1^*) - \varphi(x_2^*) > 0$ , then there are three sufficient conditions on the parameter  $c$  for the existence of a folded equilibrium of (7).
  - (a) If  $c > 2/\sqrt{3}$  then  $c - x_2^* > 0$  and  $x_1^* + x_2^* - 2c < 0$ . Therefore  $k > 0$  (by 11) and hence  $\det DH(x_1^*, x_2^*) < 0$ . Then  $(x_1^*, x_2^*)$  is a saddle of (7).
  - (b) If  $0 < c < 2/\sqrt{3}$  then  $c - x_2^* < 0$  and  $x_1^* + x_2^* - 2c < 0$ . Therefore  $k < 0$ ,  $\det DH(x_1^*, x_2^*) > 0$  and  $(x_1^*, x_2^*)$  is either a node or an unstable focus of (7).
  - (c) If  $x_1^* - c > 0$  then  $c < 0$  and  $x_1^* + x_2^* - 2c > 0$ . From (11) it follows that  $k < 0$  implying  $\det DH(x_1^*, x_2^*) > 0$  and  $(x_1^*, x_2^*)$  is either a node or an unstable focus of (7).
- (2) If  $\varphi(x_1^*) - \varphi(x_2^*) < 0$  then the conditions above on  $c$  are applicable, but  $\det DH(x_1^*, x_2^*)$  has the opposite sign as discussed above.

| region           | $x_1^*$               | $x_2^*$       | $c$                                   | other condition                   | $k$     | equilibrium type |
|------------------|-----------------------|---------------|---------------------------------------|-----------------------------------|---------|------------------|
| $\partial A_1^*$ | $x_1^* > 2/\sqrt{3}$  | $+2/\sqrt{3}$ | $c < 2/\sqrt{3}$                      | -                                 | $k > 0$ | node or focus    |
|                  |                       |               | $2/\sqrt{3} < c < (x_1^* + x_2^*)/2$  | -                                 | $k < 0$ | saddle           |
|                  |                       |               | $c > (x_1^* + x_2^*)/2$               | -                                 | $k < 0$ | node or focus    |
| $\partial A_2^*$ | $x_1^* < -2/\sqrt{3}$ | $+2/\sqrt{3}$ | $c > 2/\sqrt{3}$                      | $\varphi(x_1^*) > \varphi(x_2^*)$ | $k > 0$ | saddle           |
|                  |                       |               | $0 < c < 2/\sqrt{3}$                  | $\varphi(x_1^*) > \varphi(x_2^*)$ | $k < 0$ | node or focus    |
|                  |                       |               | $c < x_1^*$                           | $\varphi(x_1^*) > \varphi(x_2^*)$ | $k < 0$ | node or focus    |
|                  |                       |               | $c > 2/\sqrt{3}$                      | $\varphi(x_1^*) < \varphi(x_2^*)$ | $k < 0$ | node or focus    |
|                  |                       |               | $0 < c < 2/\sqrt{3}$                  | $\varphi(x_1^*) < \varphi(x_2^*)$ | $k > 0$ | saddle           |
|                  |                       |               | $c < x_1^*$                           | $\varphi(x_1^*) < \varphi(x_2^*)$ | $k > 0$ | saddle           |
| $\partial A_3^*$ | $x_1^* < -2/\sqrt{3}$ | $-2/\sqrt{3}$ | $c > -2/\sqrt{3}$                     | -                                 | $k > 0$ | node or focus    |
|                  |                       |               | $(x_1^* + x_2^*)/2 < c < -2/\sqrt{3}$ | -                                 | $k < 0$ | saddle           |
|                  |                       |               | $c < (x_1^* + x_2^*)/2$               | -                                 | $k < 0$ | node or focus    |
| $\partial A_4^*$ | $x_1^* > 2/\sqrt{3}$  | $-2/\sqrt{3}$ | $c < -2/\sqrt{3}$                     | $\varphi(x_1^*) > \varphi(x_2^*)$ | $k < 0$ | node or focus    |
|                  |                       |               | $-2/\sqrt{3} < c < 0$                 | $\varphi(x_1^*) > \varphi(x_2^*)$ | $k > 0$ | saddle           |
|                  |                       |               | $c > x_1^*$                           | $\varphi(x_1^*) > \varphi(x_2^*)$ | $k > 0$ | node or focus    |
|                  |                       |               | $c < -2/\sqrt{3}$                     | $\varphi(x_1^*) < \varphi(x_2^*)$ | $k > 0$ | saddle           |
|                  |                       |               | $-2/\sqrt{3} < c < 0$                 | $\varphi(x_1^*) < \varphi(x_2^*)$ | $k < 0$ | node or focus    |
|                  |                       |               | $c > x_1^*$                           | $\varphi(x_1^*) < \varphi(x_2^*)$ | $k < 0$ | saddle           |

TABLE 1. Sufficient conditions on  $c$  for the existence of a folded equilibrium of (7) with  $b = 0$  on the components  $\partial A_i^*$ ,  $i = 1, \dots, 4$  of the boundary of the attracting region of the critical manifold and classification of the folded equilibrium. The regions are those of Figure 1.

In the two examples shown in Figures 7 and 8, the trajectory goes near a folded node in the boundary of region  $A_3$ . The canard persists as a high frequency oscillation of small amplitude that alternates with the large amplitude relaxation oscillation of lower frequency in a *mixed-mode oscillation*. The small oscillations remain close to the synchrony plane while the large ones make alternate visits to the regions  $A_2$  and  $A_4$ . The small oscillations take place close to a double fold point, that we proceed to discuss.

**5.2. Double fold points.** In this section we deal with the dynamics around the double fold points  $X = (x_1^*, x_2^*) = (x^*, \pm x^*)$ ,  $x^* = 2\sigma/\sqrt{3}$ ,  $\sigma = \pm 1$ . We start with the equations (6) and introduce a time rescaling of  $\tau = t/\varphi'(x_1^*)\varphi'(x_2^*)$ , that is singular at  $x_i = x_i^*$ ,  $i = 1, 2$ . Then the equations (6) transform into

$$(13) \quad \begin{cases} x_1' &= \varphi'(x_2)(x_1 - (b+k)\varphi(x_1) + k\varphi(x_2) - c) &= F_1(x_1, x_2) \\ x_2' &= \varphi'(x_1)(x_2 - (b+k)\varphi(x_2) + k\varphi(x_1) - c) &= F_2(x_1, x_2). \end{cases}$$

Note that  $F_2(x_1, x_2) = F_1(x_2, x_1)$ .

Recall that we are using the notation  $A_i^*$  for the sets  $A_i^* = \{(x_1, x_2) : (x_1, x_2, \varphi(x_1), \varphi(x_2)) \in A_i\}$ ,  $i = 1, \dots, 4$ , we make the analogous convention for  $S_i^*$ ,  $i = 1, \dots, 4$  and  $R^*$  (see Figure 1). For  $(x_1, x_2) \in A_i^*$  we have  $\varphi'(x_j) < 0$ ,  $j = 1, 2$  hence the time rescaling preserves time orientation inside the  $A_i^*$ . Since  $\varphi'(x) > 0$  for  $-2/\sqrt{3} < x < 2/\sqrt{3}$  then the time rescaling also preserves time orientation in  $R^*$  and reverses it in the  $S_i^*$ ,  $i = 1, \dots, 4$ .

The main result of this section is the following:

**Theorem 5.4.** *Let  $X = (x^*, \pm x^*)$ ,  $x^* = 2\sigma/\sqrt{3}$ ,  $\sigma = \pm 1$  and let  $\phi(X) = (\varphi(x^*), \pm\varphi(x^*))$ . It is possible to have a canard for (2) near the double fold point  $(X, \phi(X))$  under the following conditions on the parameters of (2):*

- (i) for  $X = (x^*, x^*)$  (in either  $\partial A_1^*$  or  $\partial A_3^*$ ) if  $\sigma c < 2/\sqrt{3} - b\varphi(2/\sqrt{3})$ ;
- (ii) for  $X = (x^*, -x^*)$  (in either  $\partial A_2^*$  or  $\partial A_4^*$ ) if  $b + 2k < 3/8$  and  $|c| < 2/\sqrt{3} - (b + 2k)\varphi(2/\sqrt{3})$ .

There are no canards in a neighbourhood of the double fold point  $(X, \phi(X))$  under the following conditions on the parameters of (2):

- (iii) for  $X = (x^*, x^*)$  (in either  $\partial A_1^*$  or  $\partial A_3^*$ ) if  $\sigma c > 2/\sqrt{3} - b\varphi(2/\sqrt{3})$ ;
- (iv) for  $X = (x^*, -x^*)$  (in either  $\partial A_2^*$  or  $\partial A_4^*$ ) if  $b + 2k > 3/8$  and  $|c| < (b + 2k)\varphi(2/\sqrt{3}) - 2/\sqrt{3}$ .

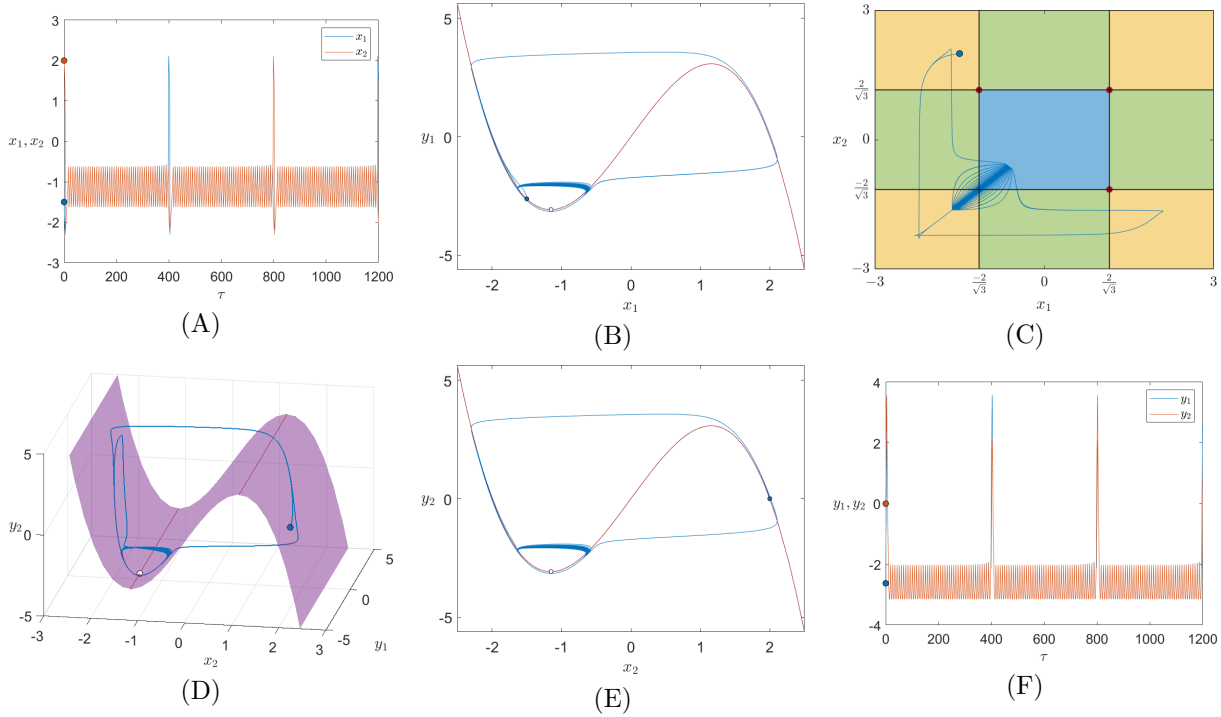


FIGURE 7. Mixed-mode oscillations arising from a canard on a solution of (2) near a folded node, parameters  $b = 0$ ,  $c = -1.150079575$ ,  $k = 1$  and  $\varepsilon = 0.5$ , initial condition  $(x_1, x_2, y_1, y_2) = (-1.5, 2, \varphi(-1.5), \varphi(2))$ . (A) - Time course for  $x_1(t)$  (blue) and  $x_2(t)$  (orange). (B) - Projection of the trajectory (blue) on the  $(x_1, y_1)$  plane, initial condition on the blue dot, red critical manifold  $C_0$ . (C) - Projection of the trajectory (red) on the  $(x_1, x_2)$  plane, initial condition on the blue dot. (D) - Projection of the trajectory (blue) on the  $(x_2, y_1, y_2)$  space, initial condition on the blue dot, purple critical manifold  $C_0$ . (E) - Projection of the trajectory (blue) on the  $(x_2, y_2)$  plane, conventions as in (B), white dot folded equilibrium. (F) - Time course for  $y_1(t)$  (blue) and  $y_2(t)$  (orange).

The parameters for the mixed-mode oscillations in Figures 7 and 8 satisfy condition (i). Note that condition (ii) only holds if  $2/\sqrt{3} - (b + 2k)\varphi(2/\sqrt{3}) > 0$  and that (iv) needs that  $2/\sqrt{3} - (b + 2k)\varphi(2/\sqrt{3}) < 0$ .

*Proof.* Let  $F(x_1, x_2) = (F_1(x_1, x_2), F_2(x_1, x_2))$  and let  $X = (x^*, \pm x^*)$ ,  $x^* = 2\sigma/\sqrt{3}$ ,  $\sigma = \pm 1$ . Since  $\varphi'(x^*) = 0$ , then  $\frac{\partial F_1}{\partial x_1}(X) = \frac{\partial F_2}{\partial x_2}(X) = 0$ . Therefore,  $\text{Tr } DF(X) = 0$  and hence, unless  $\det DF(X) = 0$ , the point  $X$  is either a saddle or a centre for the linearisation of the rescaled equations (13). A canard exists if there is a trajectory of (2) starting on the attracting part of the slow manifold  $C_\varepsilon$  that crosses the fold line into the part of  $C_\varepsilon$  that is not attracting. The idea of the proof is to show that under any of the conditions (i) and (ii) the point  $X$  is a saddle and its stable manifold intersects the corresponding  $A_i^*$ , creating the possibility of canards near  $X$ , as in [25]. For conditions (iii) and (iv) the idea is to show that although the point  $X$  is also a saddle, its stable manifold does not intersect the corresponding  $A_i^*$ , while its unstable manifold does. Hence canards are not possible around that point. We treat separately the two cases  $X = (x^*, x^*)$  and  $X = (x^*, -x^*)$ .

First, let  $X = (x^*, x^*)$ ,  $x^* = 2\sigma/\sqrt{3}$ ,  $\sigma = \pm 1$  be the double folded equilibrium of (13), lying in either  $\partial A_1^*$  or  $\partial A_3^*$ . The derivative  $DF(X)$  is given by

$$(14) \quad DF(X) = \begin{pmatrix} 0 & \varphi''(x^*)(x^* - b\varphi(x^*) - c) \\ \varphi''(x^*)(x^* - b\varphi(x^*) - c) & 0 \end{pmatrix}.$$

The matrix  $DF(X)$  is symmetric and hence its eigenvalues are real. Also

$$\det DF(X) = -(\varphi''(x^*))^2 (x^* - b\varphi(x^*) - c)^2 \leq 0$$

and hence, unless  $c = x^* - b\varphi(x^*)$ , the point  $X$  is a saddle. The eigenvalues of the matrix  $DF(X)$  are  $\lambda_1 = \varphi''(x^*)(x^* - b\varphi(x^*) - c)$  and  $\lambda_2 = -\lambda_1$  with eigenspaces  $V_1 = \{(s, s) \mid s \in \mathbf{R}\}$  and  $V_2 = \{(s, -s) \mid s \in \mathbf{R}\}$ ,

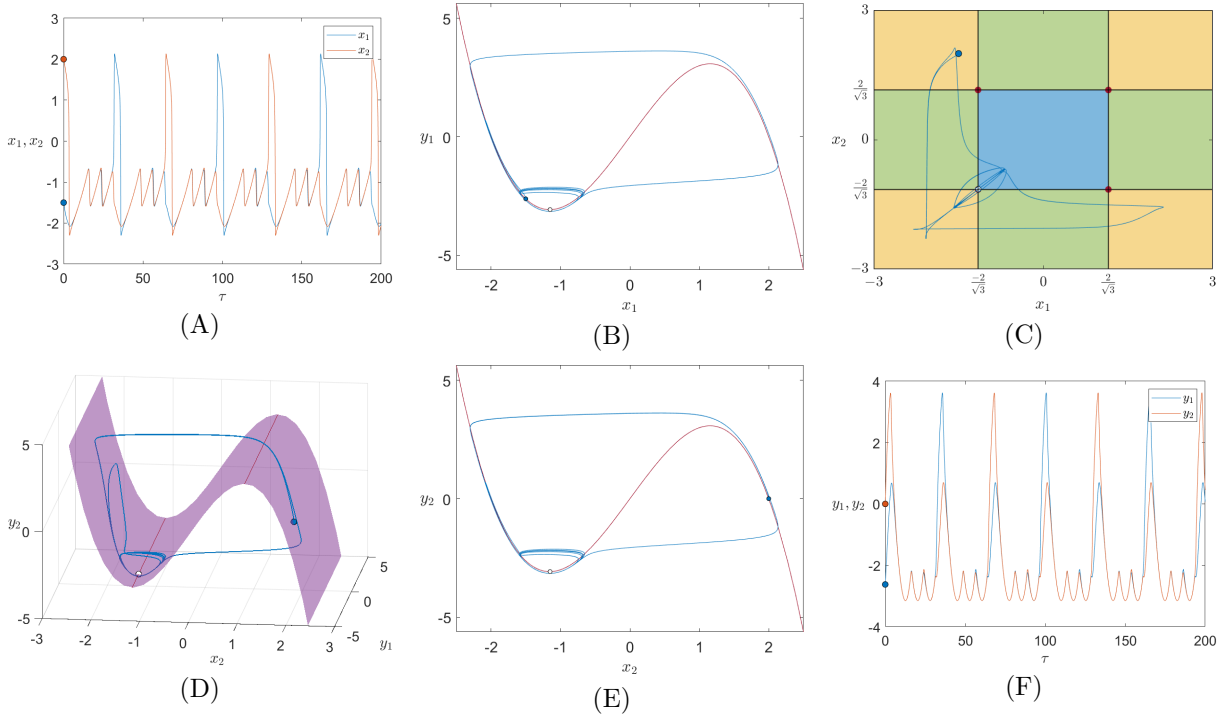


FIGURE 8. Mixed mode oscillations arising from a canard on a solution of (2) near a folded node, parameters  $b = 0$ ,  $c = -1.1501075$ ,  $k = 0.5$  and  $\varepsilon = 0.5$ , initial condition  $(x_1, x_2, y_1, y_2) = (-1.5, 2, \varphi(-1.5), \varphi(2))$ . (A) - Time course for  $x_1(t)$  (blue) and  $x_2(t)$  (orange). (B) - Projection of the trajectory (blue) on the  $(x_1, y_1)$  plane, initial condition on the blue dot, red critical manifold  $C_0$ . (C) - Projection of the trajectory (blue) on the  $(x_1, x_2)$  plane, initial condition on the blue dot. (D) - Projection of the trajectory (blue) on the  $(x_2, y_1, y_2)$  space, initial condition on the blue dot, purple critical manifold  $C_0$ . (E) - Projection of the trajectory (blue) on the  $(x_2, y_2)$  plane, conventions as in (B). (F) - Time course for  $y_1(t)$  (blue) and  $y_2(t)$  (orange).

respectively. Thus locally one of the trajectories of (13) that is tangent to  $V_1$  lies in  $A_1^*$  or  $A_3^*$ , according to the case in question and all the trajectories of (13) that are tangent to  $V_2$  lie outside  $A_1^*$  and  $A_3^*$ .

Therefore, if  $\lambda_1 < 0$  the stable manifold of  $X$  intersects the corresponding  $A_j^*$ ,  $j = 1, 3$  and canards are possible. Since for  $x^* = 2\sigma/\sqrt{3}$ ,  $\sigma = \pm 1$  the sign of  $\varphi''(x^*)$  is that of  $-\sigma$ , then  $\lambda_1 < 0$  if and only if  $\sigma c < 2/\sqrt{3} - b\varphi(2/\sqrt{3})$ . In this case then the trajectory tangent to  $V_1$  that lies in  $A_i^*$ ,  $i = 1, 3$  goes into  $X$ , so a canard is possible and assertion (i) follows.

On the other hand, if  $\lambda_1 > 0$ , then the trajectory tangent to  $V_1$  that lies in  $A_i^*$ ,  $i = 1, 3$  goes to the interior of  $A_i^*$  in positive time. Moreover, at all points near  $X$  near the boundary  $\partial A_i^*$  the vector field associated to (13) points into the interior of  $A_i^*$ . Since in both  $A_1^*$  and  $A_3^*$  the time rescaling preserves time orientation, there cannot be a canard proving assertion (iii).

Now we address the case when the double folded equilibrium of (13) is  $X = (x^*, -x^*)$ ,  $x^* = 2\sigma/\sqrt{3}$ ,  $\sigma = \pm 1$ , lying in either  $\partial A_2^*$  or  $\partial A_4^*$ . The matrix of the derivative  $DF(X)$  at  $X = (x^*, -x^*)$  is not symmetric. It is given by

$$(15) \quad DF(X) = \begin{pmatrix} 0 & -\varphi''(x^*)(x^* - (b+2k)\varphi(x^*) - c) \\ -\varphi''(x^*)(x^* - (b+2k)\varphi(x^*) + c) & 0 \end{pmatrix}$$

hence  $\text{Tr } DF(X) = 0$ , and  $\det DF(X) = -\varphi''(x^*)^2 [(x^* - (b+2k)\varphi(x^*))^2 - c^2]$ . If  $\det DF(X) > 0$  then  $DF(X)$  has a pair of purely imaginary eigenvalues. The point  $X$  is a centre for the linearisation of the desingularised equations (13). This happens when  $|c| > |(b+2k)\varphi(x^*) - x^*|$ , we do not include this situation in our analysis.

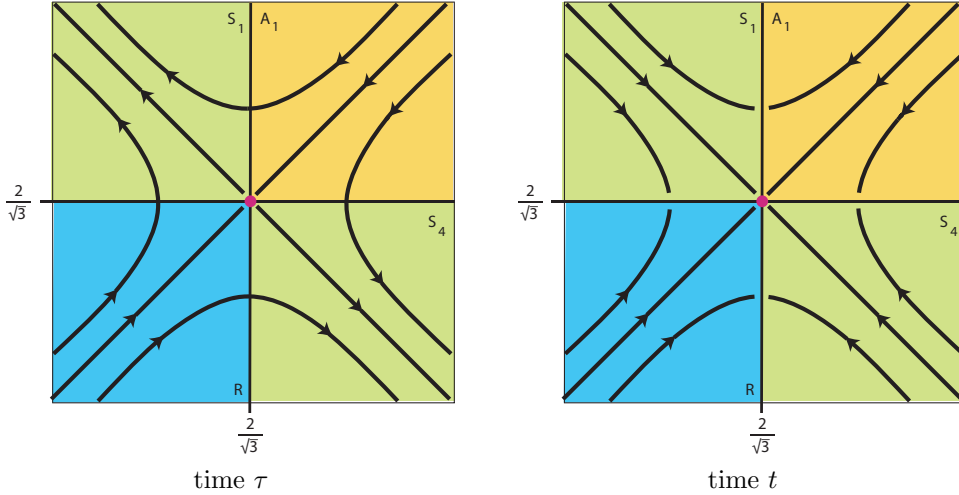


FIGURE 9. On the left, trajectories of (13) on the  $(x_1, x_2)$  plane, near the double fold point  $X = (2/\sqrt{3}, 2/\sqrt{3}) \in \partial A_1^*$  for  $\lambda_1 < 0$ , in the rescaled time  $\tau$ . On the right, trajectories of (6) near the same point, in the original time  $t$ . The rescaling inverts the time orientation in regions  $S_j$ ,  $j = 1, \dots, 4$  and preserves it in regions  $R$  and  $A_j$ ,  $j = 1, \dots, 4$ . The dynamics of (6) is not well defined when  $x_i = 2/\sqrt{3}$ ,  $i = 1, 2$ .

If  $\det DF(X) < 0$  then the point  $X$  is a saddle, since the eigenvalues of  $DF(X)$  are  $\lambda_{\pm} = \pm\sqrt{-\det DF(X)}$ . This happens if and only if

$$(16) \quad |c| < |x^* - (b + 2k)\varphi(x^*)| = \left| 2/\sqrt{3} - (b + 2k)\varphi(2/\sqrt{3}) \right|$$

and in this case the two non-zero entries in  $DF(X)$  have the same sign.

Using the same arguments of the case  $X = (x^*, x^*)$ , it is possible to have canards if one branch of the stable manifold of  $X$  lies in  $A_i^*$ ,  $i = 2, 4$ . *Canards* are not possible if the condition fails. This is determined by the directions of the eigenspace associated to the negative eigenvalue  $\lambda_-$ , which is the set  $V_- = \{(s(\alpha), \lambda_-) : s \in \mathbf{R}\}$  where  $\alpha = -\varphi''(x^*)(x^* - (b + 2k)\varphi(x^*) - c) = \frac{\partial F_1}{\partial x_2}(X)$ . There are no canards if  $\alpha < 0$ , they are possible if  $\alpha > 0$ .

It remains to show that the conditions  $\alpha > 0$  and (16) are equivalent to assertion (ii) in the statement and that  $\alpha < 0$  and (16) are equivalent to the assertion (iv).

To do this, let  $\beta = 2/\sqrt{3} - (b + 2k)\varphi(2/\sqrt{3})$ , and note that  $\alpha = -\varphi''(2/\sqrt{3})(\beta - \sigma c)$ . Since  $\varphi''(2/\sqrt{3}) = -12/\sqrt{3} < 0$  then  $\alpha$  has the same sign as  $\beta - \sigma c$ . Also note that because  $\sigma = \pm 1$  then condition (16) is equivalent to  $|\sigma c| < |\beta|$ .

If  $\beta > 0$  then condition (16) is equivalent to  $-\beta < \sigma c < \beta$  and this implies that  $\alpha > 0$ . Since  $\varphi(2/\sqrt{3}) = 16/3\sqrt{3}$  then  $\beta > 0$  if and only if  $b + 2k < 3/8$ .

If  $\beta < 0$  then condition (16) is equivalent to  $\beta < \sigma c < -\beta$  and this implies that  $\alpha < 0$ . Also  $\beta < 0$  if and only if  $b + 2k > 3/8$ .

We have established that  $\alpha > 0$  (implying canards are possible) if and only if (16) holds and  $\beta > 0$ . The necessary conditions are that  $b + 2k < 3/8$  and  $|c| < |\beta| = \beta$ , as in assertion (ii). We have also established that  $\alpha < 0$  (implying canards are not possible) if and only if (16) holds and  $\beta < 0$ , and the necessary conditions are that  $b + 2k > 3/8$  and  $|c| < |\beta| = -\beta$ , as in assertion (iv).  $\square$

In the first part of Theorem 5.4 we only claim that *canards* are possible because it is not clear that trajectories of (13) that tend to the boundary of the  $A_i^*$  correspond to trajectories of (2) that continue into  $C_0 \setminus A$ . This is because the time rescaling reverts time orientation in the  $S_i$ , the components of  $C_0$  where the equilibria of the fast equation are saddles, as shown in Figure 9. Deciding if canards exist in each case requires a detailed analysis that is beyond the scope of this article. In the special case  $b = 0$  the results of Subsection 5.1 may be used to improve the result to cover the cases shown in Figures 7 and 8.

**Theorem 5.5.** *Let  $X = (x^*, x^*)$ ,  $x^* = 2\sigma/\sqrt{3}$ ,  $\sigma = \pm 1$  be a double fold point. If  $b = 0$ ,  $k > 0$  and  $\sigma c < 2/\sqrt{3}$  then for  $\sigma c$  close to  $2/\sqrt{3}$  and small  $\varepsilon > 0$  there is a canard for (2) close to  $X$ .*

*Proof.* In Table 1 the conditions of the statement correspond to the first rows in the regions  $\partial A_1^*$  and  $\partial A_3^*$ , where the point  $(x_1^*, x_2^*)$ , with  $x_2 = x^*$  and  $\sigma x_1^* > 2/\sqrt{3}$  is either a node or a focus. The idea of the proof is to show that (a) as  $c \rightarrow 2\sigma/\sqrt{3}$  these points accumulate on  $X$ , and that (b) for  $\sigma c$  close to  $2/\sqrt{3}$  the point is a node. Then it will follow, either by Lemma 2.3 of [25], or by the results of [12] and [13], that there are solutions of (2) starting close to  $X$  in the attracting part of  $C_\varepsilon$  that follow the repelling part of  $C_\varepsilon$  for some time.

For (a) we use the fact that the restriction of the function  $\varphi(x)$  to  $\sigma x > 2/\sqrt{3}$  is a diffeomorphism. Therefore, for any  $\delta_1 > 0$  there exists a  $\delta_2 > 0$  such that if  $\sigma x_2 > 2/\sqrt{3}$  and  $|\varphi(x_1^*) - \varphi(x_2^*)| = \delta_2$ , then  $|x_1^* - x_2^*| < \delta_1$ . Using (11), if  $|c - x_2^*| < k\delta_2$  then  $|\varphi(x_1^*) - \varphi(x_2^*)| < \delta_2$  and the result follows.

For (b), we have already established in Subsection 5.1 that in this case  $\det DH(x_1^*, x_2^*) > 0$ . From the expression (12) and assertion (a) it follows that when  $c$  tends to  $2\sigma/\sqrt{3}$  then  $\det DH(x_1^*, x_2^*)$  tends to 0. Therefore, for  $c$  close to  $2\sigma/\sqrt{3}$  we have  $0 < \det DH(x_1^*, x_2^*) < 1/4$  and since  $\text{Tr } DH(x_1^*, x_2^*) = 1$ , the point  $(x_1^*, x_2^*)$  is a node.  $\square$

## 6. DISCUSSION

This article is an analysis of the dynamics of two identical FitzHugh–Nagumo equations symmetrically coupled through the slow equations. In this section we compare our results to findings by other authors using different types of coupling.

We obtain persistent synchronous (i.e. symmetric) solutions for an open set of parameters. We also show that approximate synchrony will persist if the symmetry is broken either by taking slightly different coupling constants or by a small change in the equations governing one of the cells. Synchronised periodic solutions were also observed analytically by Campbell and Waite [2] and numerically in passing by Hoff *et al.* [14] when two FHN were coupled symmetrically and bidirectionally through the fast equations, but the latter do not report on persistence under symmetry breaking, their focus being on chaotic solutions. Kawato *et al.* [15] obtain both the synchrony and its persistence for two FHN with simultaneous slow-to-slow and fast-to-fast connection. Pedersen *et al.* [22] provide bifurcation diagrams in the synchrony plane for two FHN coupled symmetrically and bidirectionally through the fast equations, showing steady-state and Hopf bifurcations that create both stable and unstable limit cycles.

The FitzHugh–Nagumo equations are symmetric when  $c = 0$ , this provides an additional symmetry to the coupled equations, with a flow-invariant fixed point subspace. From this we obtain the coexistence of different stable solutions and we show that it persists when the additional symmetry is broken for small  $c \neq 0$ . The additional symmetry does not hold when the equations are coupled through the fast equations, so this bistability is a characteristic feature of the type of coupling analysed here.

Bistability has been found in the work by Kawato *et al.* [15] coupling together the slow variables and the fast variables to each other in two FHN systems. They have obtained the coexistence of synchrony and antisynchrony through Hopf bifurcation. It has also been found by Campbell and Waite [2] who considered electrical coupling of two FHN models through the fast equation although none of these authors used the fast-slow structure. In [2] it is shown that when the magnitude of the coupling is strengthened, periodic orbits undergo several bifurcations (namely resonant Hopf-Hopf interactions) leading to the coexistence of a chaotic attractor with an attracting periodic orbit.

The symmetry in the model we have analysed limits the possible dynamic outcomes, and yet it still allows a number of interesting features. The presence of a canard induces small amplitude symmetry breaking oscillations before a solution converges to a synchronised periodic solution of large amplitude, shown in Figure 6. Santana *et al.* [24] report “transient chaos”, a complicated and long transient, in their numerical description of two FHN with different parameter values coupled through the fast equations. Canard-induced small amplitude transients were also found by Krisitiansen & Pedersen [16] in two identical FHN coupled through the fast equations. In their case the attracting periodic solution does not lie in the synchrony plane. The small amplitude transients arise from a canard at a cusp point in the critical manifold, in our case this manifold does not have cusps, so the origin of the transient oscillations is not the same, here they arise at a folded node.

Sustained mixed-mode oscillations arising from canards, like those in Figures 7 and 8, are ubiquitous in coupled FHN. They appear in asymmetric coupling of the fast equation to the slow one in Doss-Bachelet *et al.* [5] and in Krupa *et al.* [18] where three different time scales are considered. Desroches *et al.* [4] find them

in self-coupled FHN analogous to unidirectional coupling through the fast equation. Krupa *et al.* [17] find them with both the slow equations and the fast equations coupled together, when the two FHN have different parameter values. To the best of our knowledge this is the first time it appears in symmetric coupling of identical equations. The mixed-mode oscillations arise close to the point where the two fold lines cross transversely. The general analysis of the dynamics in the neighbourhood of such a point is one of the task we intend to pursue in the near future.

Because our results are based on normal hyperbolicity, they will persist under small symmetry breaking perturbations, as pointed out in Corollaries 4.4 and 4.5. However, asymmetric coupling, where one FHN is forcing the other, as in

$$(17) \quad \begin{cases} \varepsilon \dot{x}_1 &= -y_1 + \varphi(x_1) \\ \varepsilon \dot{x}_2 &= -y_2 + \varphi(x_2) \\ \dot{y}_1 &= x_1 - by_1 - c + ky_2 \\ \dot{y}_2 &= x_2 - by_2 - c \end{cases} \quad \varphi(x) = 4x - x^3 \quad b, c, k \in \mathbf{R} \quad k \neq 0$$

is not part of this scenario. Numerical evaluation of the Lyapunov spectrum of (17), presented in [14] for unidirectional coupling of two FHN through the fast equation, finds regions in the parameter space with frequency-locked solutions and other regions with chaotic behaviour. In Figure 10 we show a numerical solution of (17) that looks like a chaotic mixed-mode oscillation. This is a research direction we intend to pursue, but it is beyond the scope of the present article.

After the present study, we hope this work improves the research about theoretical and experimental applications of coupled FHN models. Possible directions should consider the importance of transient dynamics and the possibility of finding multiple attractors coexisting for the same parameter combinations. Additionally, one potential natural extension of this work is the investigation of the persistence of transient chaotic dynamics and multistability when several identical FHN models are coupled through different schemes.

#### ACKNOWLEDGMENTS

The first and second authors had financial support from CMUP, member of LASI, (UIDP/00144/2020), financed by Fundação para a Ciência e a Tecnologia, Portugal (FCT/MCTES) through national funds. The third author has been supported by the Project CEMAPRE/REM (UIDB/05069/2020) financed by FCT/MCTES through national funds.

#### REFERENCES

- [1] S. Binczak, S. Jacquir, J.-M. Bilbault, V.B. Kazantsev, V.I. Nekorkin, *Experimental study of electrical FitzHugh–Nagumo neurons with modified excitability*, Neural Networks **19** 684–693, 2006
- [2] S. A. Campbell, M. Waite, *Multistability in coupled Fitzhugh–Nagumo oscillators*, Proceedings of the Third World Congress of Nonlinear Analysts, Part 2 (Catania, 2000), Vol. 47, 2001, 1093–1104, 2001
- [3] D. Cebrián-Lacasa, P. Parra-Rivas, D. Ruiz-Reynés, L. Gelens, *Six decades of the FitzHugh–Nagumo model: A guide through its spatio-temporal dynamics and influence across disciplines* arXiv: 2404.11403v3 [nlin.PS], 2024
- [4] M. Desroches, B. Krauskopf, H. Osinga, *Mixed-mode oscillations and slow manifolds in the self-coupled FitzHugh–Nagumo system*, Chaos **18** 015107, 2008
- [5] C. Doss-Bachelet, J.-P. François, C. Piquet, *Bursting oscillations in two coupled FitzHugh–Nagumo systems* ComplexUs, **1(3)**01–111, 2003
- [6] N. Fenichel, *Persistence and Smoothness of Invariant Manifolds for Flows*, Indiana University Mathematics Journal, **21(3)** 193–226, 1971
- [7] N. Fenichel, *Geometric singular perturbation theory for ordinary differential equations*, Journal of Differential Equations **31(1)** 53–98, 1979
- [8] R. FitzHugh, *Thresholds and plateaus in the Hodgkin–Huxley nerve equations*, Journal of General Physiology **43 no. 5** 867–896, 1960
- [9] R. Fitzhugh, *Impulses and physiological states in theoretical models of nerve membrane*, Biophysical Journal **1 no. 6** 445–466, 1961
- [10] B.F.F. Gonçalves, I.S. Labouriau, A.A.P. Rodrigues, *Bifurcations and canards in the FitzHugh–Nagumo system: a tutorial of fast-slow dynamics* arXiv: 2411.11209v1, 2024 to appear in International Journal of Bifurcation and Chaos
- [11] W. Govaerts, Yu. A. Kuznetsov, H. G. E. Meijer, B. Al-Hdaibat, V. De Witte, A. Dhooge, W. Mestrom, N. Neiryck, A. M. Riet, and B. Sautois, *Matcont: Continuation toolbox for odes in matlab*, 2019.
- [12] J. Guckenheimer, R. Haiduc, *Canards at folded nodes*, Moscow Mathematical Journal **5 no. 1** 91–103, 2005
- [13] J. Guckenheimer, *Return maps of folded nodes and folded saddles*, Chaos **8** 015108, 2008
- [14] A. Hoff, J. V. dos Santos, C. Manchein, H. A. Albuquerque, *Numerical bifurcation analysis of two coupled FitzHugh–Nagumo oscillators*, Eur. Phys. J. B **87**: 151, 2014



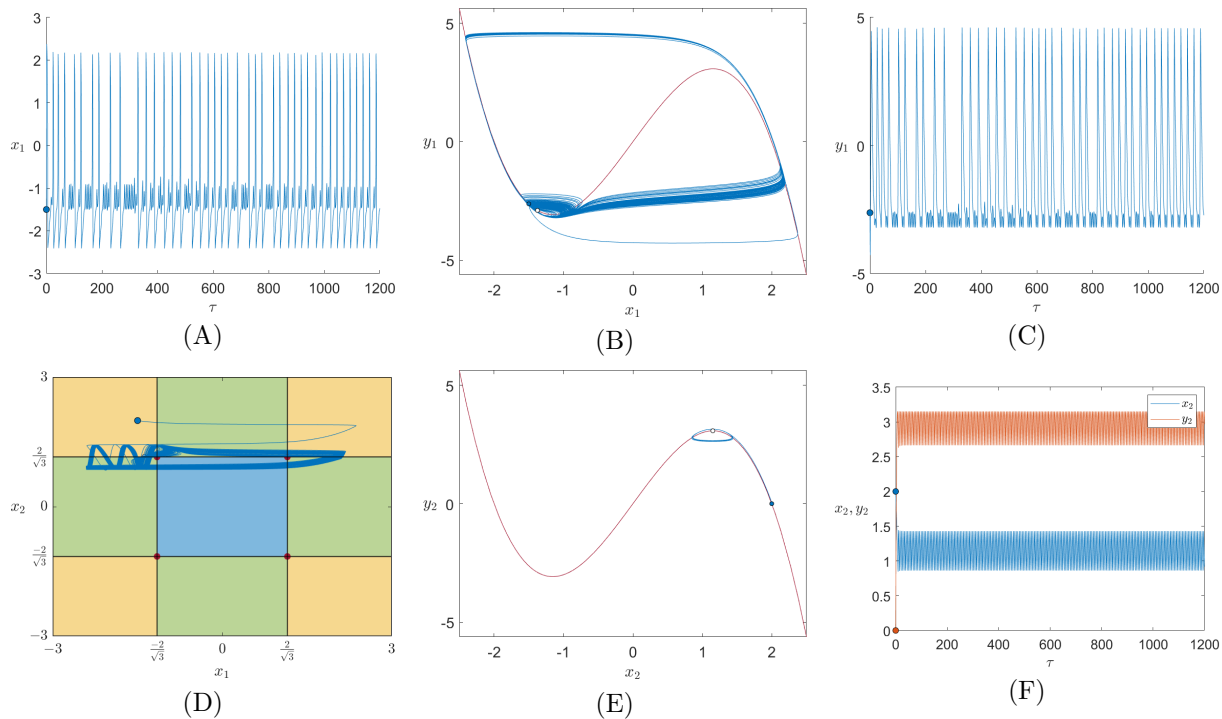


FIGURE 10. Chaotic mixed-mode oscillations in (17), parameters  $b = 0$ ,  $c = 1.1505466726$ ,  $k = 0.820125$  and  $\varepsilon = 0.5$ , initial condition  $(x_1, x_2, y_1, y_2) = (2, 2, 0, 0)$ . (A) - Time course for  $x_1(t)$ . (B) - Projection of the trajectory (blue) on the  $(x_1, y_1)$  plane, initial condition on the blue dot, red critical manifold  $C_0$ . (C) - Time course for  $y_1(t)$ .

(D) - Projection of the trajectory (blue) on the  $(x_1, x_2)$  plane, initial condition on the blue dot. (E) - Projection of the trajectory (blue) on the  $(x_2, y_2)$  plane, initial condition on the blue dot, red critical manifold  $C_0$ , equilibrium on the white dot. (F) - Time course for  $x_2(t)$  (blue) and  $y_2(t)$  (orange).

- [15] M. Kawato, M. Sokabe, M. Suzuki, *Synergism and Antagonism of Neurons Caused by an Electrical Synapse*, Biol. Cybernetics **34** 81–89, 1979
- [16] K.U. Kristiansen, M.G. Pedersen, *Mixed-mode oscillations in coupled FitzHugh–Nagumo oscillators: blow-up analysis of cusped singularities*, SIAM J. Appl. Dyn. Syst. **22** (2) 1383–1422 2023
- [17] M. Krupa, B. Ambrosio, M.A. Aziz–Alaoui, *Weakly coupled two–slow–two–fast systems, folded singularities and mixed mode oscillations*, Nonlinearity **27** 1555–1574, 2014
- [18] M. Krupa, A. Vidal, M. Desroches, F. Clément, *Mixed-mode oscillations in a multiple time scale phantom bursting system*, SIAM J. Applied Dynamical Systems, **11**(4) 1458–1498, 2012
- [19] C. Kuehn, *Multiple time scale dynamics*, Springer-Verlag 2015
- [20] I.S. Labouriau, H.M. Rodrigues, *Synchronization of coupled equations of Hodgkin-Huxley type*, Dynamics of Continuous Discrete and Impulsive Systems — Series A — Mathematical Analysis **10**, 463–476, 2003
- [21] J. Nagumo, S. Arimoto, and S. Yoshizawa, *An active pulse transmission line simulating nerve axon*, Proceedings of the IRE **50**, no. **10**, 2061–2070, 1962
- [22] M. G. Pedersen, M. Brøns, and M. P. Sørensen, *Amplitude-modulated spiking as a novel route to bursting: Coupling-induced mixed- mode oscillations by symmetry breaking*, Chaos, **32** 013121, 2022
- [23] A. Saha, U. Feudel, *Extreme events in FitzHugh–Nagumo oscillators coupled with two time delays*, Phys. Rev. E, **95** 062219, 2017. doi: 10.1103/PhysRevE.95.062219
- [24] L. Santana, R.M. da Silva, H.A. Albuquerque, C. Manchein, *Transient dynamics and multistability in two electrically interacting FitzHugh–Nagumo neurons* Chaos **31** 053107, 2021
- [25] P. Szmolyan, M. Wechselberger, *Canards in  $\mathbf{R}^3$* , Journal of Differential Equations **177** (2) 419–453, 2001

B.F.F. GONÇALVES — CENTRO DE MATEMÁTICA DA UNIVERSIDADE DO PORTO, RUA DO CAMPO ALEGRE, 687, 4169-007 PORTO, PORTUGAL

*Email address:* B.F.F. Gonçalves --- brunoffg9@gmail.com

I.S. LABOURIAU — CENTRO DE MATEMÁTICA DA UNIVERSIDADE DO PORTO, RUA DO CAMPO ALEGRE, 687, 4169-007 PORTO, PORTUGAL

*Email address:* I.S. Labouriau --- islabour@fc.up.pt

A.A. P. RODRIGUES — LISBON SCHOOL OF ECONOMICS & MANAGEMENT, CENTRO DE MATEMÁTICA APLICADA À PREVISÃO E DECISÃO ECONÓMICA, RUA DO QUELHAS 6, 1200-781, LISBOA, PORTUGAL

*Email address:* A.A. P. Rodrigues --- arodrigues@iseg.ulisboa.pt